

Regular article

Estimating bounds on the highest and lowest eigenvalues of any matrix

Srinivasan S. Iyengar^{1*}, Donald J. Kouri¹, Gregory A. Parker², David K. Hoffman³

¹Department of Chemistry and Department of Physics, University of Houston, Houston, TX 77204-5641, USA

²Department of Physics and Astronomy, University of Oklahoma, Norman, OK 73019, USA

³Department of Chemistry and Ames Laboratory, Iowa State University, Ames, IA 50011, USA

Received: 7 May 1999 / Accepted: 30 July 1999 / Published online: 15 December 1999

© Springer-Verlag 2000

Abstract. A method for estimating the bounds for the highest and lowest eigenvalues of a finite-dimensional matrix is presented. The method is tested for the Hamiltonian matrix for several particle-in-a-box-like systems. We also provide results for the well-studied benchmark case of the ro-vibrational states of H_3^+ , and consider bounds obtained for a completely random non symmetric matrix. Finally, we discuss how the error in a Chebychev expansion solution of quantum scattering depends on the error made in estimating the highest eigenvalue of the Hamiltonian matrix.

Key words: Chebychev expansion of Green's functions – Normalizing matrices – Upper bounds of eigenvalues – Truncation errors

1 Introduction

Normalizing a matrix so that it has eigenvalues only on the range $[-1, +1]$ is required in a number of areas of physical sciences [1–16]. In quantum mechanics, wave-packet propagation using the Chebychev polynomial expansion for Green's function [11, 12, 17], the spectral density operator [4, 5] or the evolution operator requires a normalized Hamiltonian matrix [1–3]; therefore, it is of interest to obtain good estimates of the upper and lower bounds of the eigenvalue spectrum of the Hamiltonian matrix. For example, one expects the quality of this estimation to affect the convergence properties of Chebychev expansions, with a “tighter” bound leading to faster convergence. Direct methods for solving eigenvalue problems and linear systems of equations,

such as QR factorization, are also sensitive to the range of the eigenvalue spectrum.

This paper is organized as follows. In Sects. 2 and 3, we review the concept of norms and how the upper bound for the L^2 norm can be used to obtain an upper bound for the highest eigenvalue and a lower bound for the lowest eigenvalue in the spectrum of any matrix. In Sect. 4, we present analytical expressions showing how the remainder from the truncation of the Chebychev expansion depends on the error in estimating the Hamiltonian matrix upper bound and briefly discuss the computational scaling of the algorithm. In Sect. 5, we present some calculations done using the results from Sects. 2 and 3 and compare these results with those obtained from a widely used, existing approach. We present our conclusions in Sect. 6.

2 Norm basics

Following the ideas discussed in Ref. [18], we present here some definitions which are used in Sect. 3 to obtain estimates for the upper and lower bounds for the eigenvalue spectrum of any matrix.

The L^p norm of a vector, \mathbf{x} , is defined to be

$$\|\mathbf{x}\|_p \equiv \left[\sum_{i=1}^n |x_i|^p \right]^{\frac{1}{p}}, \quad (1)$$

where n is the dimensionality of the vector. Specifically, the L^1 , L^2 and L^∞ norms of a vector \mathbf{x} are given respectively by

$$\|\mathbf{x}\|_1 = \left[\sum_{i=1}^n |x_i| \right], \quad (2)$$

$$\|\mathbf{x}\|_2 = \left[\sum_{i=1}^n |x_i|^2 \right]^{\frac{1}{2}} \quad (3)$$

and

* Present address:

Department of Chemistry, Rice Quantum Institute
and Center for Nanoscale Science and Technology,
Mail Stop 60, Rice University, Houston, TX 77005-1892, USA

Correspondence to: D.J. Kouri

$$\|x\|_\infty = \max_{1 \leq i \leq n} |x_i| . \quad (4)$$

The L^p norm of an $m \times n$ rectangular (complex) matrix, \mathbf{A} , is defined to be the L^p norm of the vector, having the largest L^p norm, that is obtained by applying \mathbf{A} to vectors, \mathbf{x} , with unit L^p norm, i.e.,

$$\|A\|_p \equiv \max_{\|x\|_p=1} \|Ax\|_p . \quad (5)$$

Using these relations it can be shown that the L^1 and L^∞ norms of the $m \times n$ matrix \mathbf{A} are

$$\|A\|_1 = \max_{1 \leq j \leq n} \sum_{i=1}^m |A_{ij}| \quad (6)$$

and

$$\|A\|_\infty = \max_{1 \leq i \leq m} \sum_{j=1}^n |A_{ij}| . \quad (7)$$

Equations (6) and (7) are derived in Appendix 1.

Consider, now, the $n \times n$ Hermitian matrix $\mathbf{A}^\dagger \mathbf{A}$. Since $(\mathbf{x}^\dagger \mathbf{A}^\dagger \mathbf{A} \mathbf{x}) \geq 0$ for any vector \mathbf{x} , it follows that the eigenvalues of $\mathbf{A}^\dagger \mathbf{A}$ are non negative. Further, from Eqs. (3) and (5), it follows that

$$\|A\|_2 = \max_{\|x\|_2=1} \|Ax\|_2 = \max_{\|x\|_2=1} \sqrt{(\mathbf{x}^\dagger \mathbf{A}^\dagger \mathbf{A} \mathbf{x})} , \quad (8)$$

and hence that the square root of the largest eigenvalue of $\mathbf{A}^\dagger \mathbf{A}$ is the L^2 norm of \mathbf{A} . That is,

$$\mathbf{A}^\dagger \mathbf{A} \mathbf{z} = |\mu|^2 \mathbf{z} , \quad (9)$$

where $|\mu|$ is the L^2 norm (and the largest absolute eigenvalue) of \mathbf{A} and \mathbf{z} is the corresponding eigenvector of $\mathbf{A}^\dagger \mathbf{A}$.

An upper bound for the L^2 norm of \mathbf{A} can be obtained from

$$\|A\|_2 \leq \sqrt{\|A\|_1 \|A\|_\infty} . \quad (10)$$

(A proof of this expression, together with other relations involving the various norms is given in Appendix 2.) Since the L^1 norm and the L^∞ norm just correspond to maximum sums of columns and rows respectively, an upper bound for the L^2 norm, i.e., an upper bound for the maximum absolute eigenvalue of the matrix \mathbf{A} is quite easy to calculate from Eq. (10), as will be seen in the next section.

3 Estimating the bounds of a matrix

As discussed in the introductory section, it is useful in a number of situations to have bounds for the spectrum of a matrix, and as is to be anticipated, in virtually every application, the ‘‘tighter’’ these bounds can be determined, the better. A number of ways to estimate such bounds exists [19–26]. In this section we explore a method based on the relations of the L^2 norm to the upper and lower bounds of the eigenvalue spectrum of any matrix.

Consider a finite matrix, \mathbf{H} , for which we wish to obtain spectral bounds. We begin by first constructing

the matrix \mathbf{A} of Sect. 1 as a function of \mathbf{H} i.e., $\mathbf{A} \equiv \mathbf{A}(\mathbf{H})$, in such a way that the norm of \mathbf{A} is simply related to the spectrum of \mathbf{H} . An example which we will examine in some detail is

$$\mathbf{A} = \mathbf{H} - c\mathbf{I} , \quad (11)$$

where \mathbf{I} is the unit matrix and c is an arbitrary scalar constant. A more general version may be obtained by replacing $c\mathbf{I}$ in Eq. (11) by any matrix, \mathbf{B} , so that

$$\mathbf{A} = \mathbf{H} - \mathbf{B} , \quad (12)$$

where the commutator $[\mathbf{H}, \mathbf{B}] = 0$. In the case of Eq. (11) eigenvalues of \mathbf{A} and \mathbf{H} are, of course, simply related by the additive constant, c . From Sect. 2, we know that the L^2 norm of \mathbf{A} is the largest absolute eigenvalue of \mathbf{A} and hence that

$$-\|A\|_2 + c \leq \mathcal{E}(H) \leq \|A\|_2 + c , \quad (13)$$

where $\mathcal{E}(H)$ is the spectrum of \mathbf{H} . Clearly, for $c \geq \frac{\lambda_{\max} + \lambda_{\min}}{2}$ the lower bound is exact, and for $c \leq \frac{\lambda_{\max} + \lambda_{\min}}{2}$ the upper bound is exact (λ_{\max} and λ_{\min} being the unknown maximum and minimum eigenvalues of \mathbf{H} , respectively). Using Eq. (10) it immediately follows that

$$c - \sqrt{\|A\|_1 \|A\|_\infty} \leq \mathcal{E}(H) \leq c + \sqrt{\|A\|_1 \|A\|_\infty} . \quad (14)$$

For a value of c sufficiently above the midpoint of the spectrum we expect the lower bound estimate to be ‘‘tighter’’ and vice versa for c sufficiently below the midpoint.

To explore the structure of the bounds in Eq. (14), consider the quantity

$$\sum_i |A_{ij}| = |H_{jj} - c| + \sum_{i \neq j} |H_{ij}| \quad (15)$$

as a function of c for fixed j . It consists of two line segments, one with slope $+1$ and the other with slope -1 . These lines intersect at $c = H_{jj}$, at which point the function has the values $\sum_{i \neq j} |H_{ij}|$. For values of c greater than all the diagonal elements of \mathbf{H} , the quantity $\sum_i |A_{ij}|$, for all possible values of j , is a set of parallel lines of slope $+1$. Likewise, for values of c less than all the diagonal elements of \mathbf{H} , the quantity $\sum_i |A_{ij}|$, for all j , comprises a set of lines with slope -1 . Let j_R label the highest lying line for large c and j_L label the highest lying line for large negative c . These lines intersect at $c = \alpha$, where

$$\alpha - H_{j_R j_R} + \sum_{i \neq j_R} |H_{ij_R}| = H_{j_L j_L} - \alpha + \sum_{i \neq j_L} |H_{ij_L}| , \quad (16)$$

or

$$\alpha = \frac{1}{2} \left[H_{j_R j_R} + H_{j_L j_L} + \sum_{i \neq j_L} |H_{ij_L}| - \sum_{i \neq j_R} |H_{ij_R}| \right] . \quad (17)$$

The value of the lines at this intersection,

$$\beta = \frac{1}{2} \left[H_{j_L j_L} - H_{j_R j_R} + \sum_{i \neq j_L} |H_{ij_L}| + \sum_{i \neq j_R} |H_{ij_R}| \right] , \quad (18)$$

is clearly a positive quantity since $H_{j_L j_L} \geq H_{j_R j_R}$. The L^1 norm of \mathbf{A} as a function of c then is of the form

$$\|A\|_1 = |c - \alpha| + \beta, \quad (19)$$

since it is impossible for $\sum_i |A_{ij}|$ to intersect this curve for any j other than j_R and j_L , if these indices correspond to the highest lying lines as previously discussed. Precisely the same argument holds for $\|A\|_\infty$, except in this case the sum is over the columns of \mathbf{H} rather than the rows.

From this analysis it is seen that the upper and lower bounds in Eq. (14) assume the form

$$c \pm \sqrt{\|A\|_1 \|A\|_\infty} = c \pm \sqrt{(|c - \alpha_1| + \beta_1)(|c - \alpha_2| + \beta_2)}, \quad (20)$$

where α_1, β_1 are the constants corresponding to $\|A\|_1$ and α_2, β_2 correspond to $\|A\|_\infty$ or vice versa. If, for the sake of concreteness, we assume $\alpha_2 \geq \alpha_1$, the explicit upper and lower bounds are then given by

$$c \pm \sqrt{(\alpha_1 - c + \beta_1)(\alpha_2 - c + \beta_2)}, \quad c \leq \alpha_1, \quad (21)$$

$$c \pm \sqrt{(c - \alpha_1 + \beta_1)(\alpha_2 - c + \beta_2)}, \quad \alpha_1 < c < \alpha_2, \quad (22)$$

and

$$c \pm \sqrt{(c - \alpha_1 + \beta_1)(c - \alpha_2 + \beta_2)}, \quad c \geq \alpha_2. \quad (23)$$

For a self-adjoint (Hermitian) matrix, \mathbf{H} , $\alpha_1 = \alpha_2$ (since, in this case $\|A\|_1 = \|A\|_\infty$), and the region given by Eq. (22) collapses to a point leaving only two possible regions. Furthermore, at $c = \alpha_1$, the expressions in Eqs. (21) and (22) are equal, and similarly at $c = \alpha_2$, the expressions in Eqs. (22) and (23) are equal. Hence the upper and lower bounds in Eq. (14) are continuous functions of c .

By considering the slopes of the upper and lower bounds in the three regions previously described, it is easily shown that the greatest lower bound and the least upper bound can be obtained either at $c = \alpha_1$ or at $c = \alpha_2$. (A proof of this may be found in Appendix 3.)

For the self-adjoint case, as already shown, the central region collapses to a point, and both bounds occur at $c = \alpha_1 = \alpha_2$. In this case the greatest lower bound is

$$H_{j'j'} - \sum_{\substack{i=1 \\ i \neq j'}}^n |H_{ij'}|, \quad (24)$$

where j' labels the column for which this expression is a minimum. Similarly, the least upper bound for this case is

$$H_{j''j''} + \sum_{\substack{i=1 \\ i \neq j''}}^n |H_{ij''}|, \quad (25)$$

where now j'' is the index for which the expression is a maximum. It should be noted that Eqs. (24) and (25) have the exact same form as the upper and lower bounds obtained from Gerschgorin's disk theorem [27, 28]¹. For non-Hermitian matrices, however, one obtains expressions that are different from those due to Gerschgorin's disk theorem, as seen from the discussion in this section.

It is interesting to compare these results with the $c = 0$ case (i.e., $\mathbf{A} = \mathbf{H}$), for which the upper and lower bounds are given by

$$\pm \left(|H_{j''j''}| + \sum_{\substack{i=1 \\ i \neq j''}}^n |H_{ij''}| \right). \quad (26)$$

Equations (24)–(26) are, of course, similar in form and, depending on the diagonal elements, can be the same; however, for any value of j the sequence of inequalities

$$\begin{aligned} \left(-|H_{jj}| - \sum_{\substack{i=1 \\ i \neq j}}^n |H_{ij}| \right) &\leq \left(H_{jj} - \sum_{\substack{i=1 \\ i \neq j}}^n |H_{ij}| \right) \\ &\leq \left(H_{jj} + \sum_{\substack{i=1 \\ i \neq j}}^n |H_{ij}| \right) \leq \left(|H_{jj}| + \sum_{\substack{i=1 \\ i \neq j}}^n |H_{ij}| \right) \end{aligned} \quad (27)$$

holds. They show explicitly that the upper and lower bounds of the expression in Eq. (26) are, at best, only as good as and never better than those of Eqs. (24) and (25), respectively (which, of course, must be the case from our more general considerations).

The results of the preceding discussion lead immediately to an algorithm for obtaining upper and lower bounds for the spectrum of \mathbf{H} . For a self-adjoint matrix, the lower and upper bounds are given by

$$\min_j \left[H_{jj} - \sum_{i \neq j} |H_{ij}| \right] \text{ and } \max_j \left[H_{jj} + \sum_{i \neq j} |H_{ij}| \right],$$

respectively, whereas for a non-self-adjoint matrix, they are to be determined at values of c equal to α_1 and α_2 .

Another set of bounds on the spectrum of \mathbf{H} can always be obtained by writing the matrix as a sum of two (or more) other matrices, for example, for the Hamiltonian, $\mathbf{H} = \mathbf{T} + \mathbf{V}$, where \mathbf{T} is the kinetic energy (KE) and \mathbf{V} is the potential. It is clear that $(\mathbf{x}^\dagger \mathbf{T} \mathbf{x})$, for any (L^2) normalized vector \mathbf{x} , must be less than or equal to the largest eigenvalue of \mathbf{T} , and similarly for \mathbf{V} . Hence, the sum of the largest eigenvalues of \mathbf{T} and of \mathbf{V} must provide an upper bound for the spectrum of \mathbf{H} . Similarly, the sum of the two lowest eigenvalues of \mathbf{T} and \mathbf{V} must provide a lower bound for the spectrum of \mathbf{H} . (The quality of these bounds will, of course, depend on the "size" of the commutator $[\mathbf{T}, \mathbf{V}]$.) This observation can be useful if \mathbf{T} and \mathbf{V} are each either diagonalized easily or bounds to their respective spectra are obtained easily. For a matrix representing the Hamiltonian operator, typically bounds of this kind are easily obtained and are often employed in quantum mechanical calculations [7, 9, 17]. The KE operator is often represented either by a finite circulant matrix or a particle-in-a-box matrix, and the (local) potential energy (PE) operator by a diagonal matrix, and the spectral bounds are trivially obtained in either case. For the Hamiltonian matrix, the lower bound established in this manner is better than the upper bound because there is a physical lower bound to the spectrum of the operators corresponding to these finite matrices (i.e., zero in the case of the KE operator and the minimum on the PE surface in the case of the PE operator).

¹ We thank Stephan Grey for bringing this to our attention

In cases where the spectral bounds for \mathbf{T} are not easily obtained, an approximation to highest (lowest) eigenvalue of \mathbf{T} summed with the maximum (minimum) value of the local potential on a grid may be used as an upper bound (lower bound) for the eigenvalue spectrum of \mathbf{H} .

Another method is to accurately determine the highest and lowest eigenvalues of \mathbf{H} using a Lanczos or Arnoldi procedure [18, 29–31]. In both methods, repetitive application of the matrix, \mathbf{H} , to an initial (sometimes random) vector produces a Krylov basis set [18]; the representation of the original matrix in this new basis set leads to a Hessenberg form if the matrix \mathbf{H} is non-Hermitian and to a tridiagonal form if the matrix \mathbf{H} is Hermitian [18], both of which can be easily diagonalized. This method is known to converge rapidly to the external (i.e., largest and smallest) eigenvalues [18].

4 Effect of error in and computational cost of the upper bound estimate

It is of some interest and importance to know the manner in which the convergence of the Chebychev expansion of Green's function, the time evolution operator, or the Dirac delta function depends on the accuracy of the upper bound estimate. In fact, this can be determined using an expression derived for the truncation error presented in our earlier work [16]:

$$R_m(E) = \frac{\Delta H}{2} [T_m(E_{\text{norm}})T_{m+1}(H_{\text{norm}}) - T_{m+1}(E_{\text{norm}})T_m(H_{\text{norm}})]\chi(0) , \quad (28)$$

where the series is truncated at the m th Chebychev, E_{norm} and H_{norm} are the normalized collision energy and Hamiltonian matrix, given by

$$E_{\text{norm}} = (\mathbf{E} - \bar{H})/2 , \quad (29)$$

$$H_{\text{norm}} = (\mathbf{H} - \bar{H})/2 , \quad (30)$$

and the exact spectral range, ΔH , and the arithmetic average of the highest and lowest eigenvalues, \bar{H} , are respectively

$$\Delta H = (E_{\text{max}} - E_{\text{min}})/2 , \quad (31)$$

$$\bar{H} = (E_{\text{max}} + E_{\text{min}})/2 , \quad (32)$$

and $E_{\text{max}}(E_{\text{min}})$ is the exact maximum (minimum) eigenvalue of the Hamiltonian matrix. The quantity $\chi(0)$ is the initial wavepacket associated with the experiment of interest, so $R_m(\mathbf{E})$ is a state vector which in the coordinate representation depends on both the scattering and internal variables. It is convenient to expand $\chi(0)$ in the basis of eigenstates of the matrix Hamiltonian,

$$H\psi_\lambda = E_\lambda\psi_\lambda , \quad (33)$$

so that

$$\chi(0) = \sum_\lambda A_\lambda\psi_\lambda . \quad (34)$$

Then the truncation error at the m th Chebychev term, projected onto the λ th eigenstate, with exactly normalized arguments is

$$[R_m(E)]_\lambda = \frac{\Delta H A_\lambda}{2} [T_m(E_{\text{norm}})T_{m+1}(E_{\lambda,\text{norm}}) - T_{m+1}(E_{\text{norm}})T_m(E_{\lambda,\text{norm}})] , \quad (35)$$

where $E_{\lambda,\text{norm}} = (E_\lambda - \bar{H})/\Delta H$. We focus on the effect of the upper bound estimate and assume the lower bound is exactly zero. The upper bound is estimated as $E_{\text{max}} + \eta$, where we assume that η is positive (an estimate of the upper bound that is less than the true upper bound leads to divergence of the Chebychev expansion). Then we denote the truncation remainder, when the upper bound is in error by η , by

$$[\tilde{R}_m(E)]_\lambda = \frac{\Delta H A_\lambda}{2} [T_m(\tilde{E}_{\text{norm}})T_{m+1}(\tilde{E}_{\lambda,\text{norm}}) - T_{m+1}(\tilde{E}_{\text{norm}})T_m(\tilde{E}_{\lambda,\text{norm}})] , \quad (36)$$

where

$$\tilde{H} \equiv \tilde{\Delta H} = (E_{\text{max}} + \eta)/2 , \quad (37)$$

and

$$\tilde{E}_{\text{norm}} = \frac{2E - (E_{\text{max}} + \eta)}{(E_{\text{max}} + \eta)} , \quad (38)$$

$$\tilde{E}_{\lambda,\text{norm}} = \frac{2E_\lambda - (E_{\text{max}} + \eta)}{(E_{\text{max}} + \eta)} . \quad (39)$$

Then the error, at the same level of truncation of the Chebychev series, is given by

$$[\Delta R_m(E)]_\lambda \equiv [\tilde{R}_m(E)]_\lambda - [R_m(E)]_\lambda . \quad (40)$$

Clearly, substituting for the two remainders leads to very messy algebra. A better way to proceed is to use the expression for $[\tilde{R}(E)]_\lambda$ to derive a differential equation for the rate of change of the remainder with the upper bound error, η . This is, in fact, easily done and we simply quote the result:

$$\frac{d[\tilde{R}_m(E)]_\lambda}{d\eta} = \frac{[\tilde{R}_m(E)]_\lambda}{(E_{\text{max}} + \eta)} + q(\eta) , \quad (41)$$

where

$$q(\eta) \equiv \frac{(E_{\text{max}} + \eta)A_\lambda}{8} \left\{ - \left(\frac{mE}{E(E_{\text{max}} + \eta) - E^2} \right) \times [T_{m-1}(\tilde{E}_{\text{norm}}) - T_m(\tilde{E}_{\text{norm}})]T_{m+1}(\tilde{E}_{\lambda,\text{norm}}) - \left(\frac{E_\lambda(m+1)}{E_\lambda(E_{\text{max}} + \eta) - E^2} \right) \times [T_m(\tilde{E}_{\lambda,\text{norm}}) - T_{m+1}(\tilde{E}_{\lambda,\text{norm}})]T_m(\tilde{E}_{\text{norm}}) + \left(\frac{E(m+1)}{E(E_{\text{max}} + \eta) - E^2} \right) \times [T_m(\tilde{E}_{\text{norm}}) - T_{m+1}(\tilde{E}_{\text{norm}})]T_m(\tilde{E}_{\lambda,\text{norm}}) + \left(\frac{E_\lambda m}{E_\lambda(E_{\text{max}} + \eta) - E_\lambda^2} \right) \times [T_{m-1}(\tilde{E}_{\lambda,\text{norm}}) - T_m(\tilde{E}_{\lambda,\text{norm}})]T_{m+1}(\tilde{E}_{\text{norm}}) \right\} . \quad (42)$$

(The derivation of the above result involves use of the chain rule for ordinary derivatives and the recursion expressing the derivative of a Chebychev polynomial in terms of a difference of these polynomials.)

There are several special cases of interest. The first is when the energy $E \equiv E_\lambda$, in which case the inhomogeneity $q(\eta)$ is identically zero and the solution of the resulting first-order, linear homogeneous ordinary differential equation is

$$[\tilde{R}_m(E_\lambda)]_\lambda = [R_m(E_\lambda)]_\lambda \left(1 + \frac{\eta}{E_{\max}}\right). \quad (43)$$

One also obtains the same result when $\mathbf{E} \equiv \mathbf{E}_{\max}$, since this is simply the largest of the eigenvalues of the matrix \mathbf{H} . In these cases, the error in the λ th component of the remainder due to overestimating E_{\max} by η is linear in η/E_{\max} . Of course, the error for the components other than the λ th will involve contributions from the inhomogeneity, $q(\eta)$, and these are, in general, nonlinear in η . The most general case is very messy and we have evaluated it only for some special values of m . The results indicate that the leading nonlinear term depends on η/E_{\max} logarithmically. As a result, the dominant term appears to be the linear one.

Finally, we briefly discuss the computational scaling for the bound calculation outlined in Sect. 3. For the case of a self-adjoint matrix, the greatest lower bound is

given by $\min_j \left[H_{jj} - \sum_{i \neq j} |H_{ij}| \right]$ and the least upper bound is given by $\max_j \left[H_{jj} + \sum_{i \neq j} |H_{ij}| \right]$. Calculating each of

these for an $N \times N$ matrix requires $N(N-1)$ additions, $(N-1)$ comparisons and no multiplications. Hence, the computational time required to perform this calculation is roughly proportional to N^2 additions (for large N). For the non-self-adjoint case, it is first necessary to obtain j_R and j_L (in Eqs. 16–18), which are used to get α_1 , α_2 , β_1 and β_2 . Following this, one may obtain the upper and lower bounds, as outlined. To calculate j_R and j_L requires $2N(N-1)$ additions, $(N-1)$ comparisons and no multiplications. α_1 , α_2 , β_1 and β_2 can then be calculated using $8N$ additions. The calculation of the bounds can be achieved with another four multiplications, four additions, four square-root operations and two comparisons (i.e., the number of multiplications and square-root operations are independent of N). Thus a total of $(2N^2 + 6N + 4)$ additions, $(N+1)$ comparisons, four multiplications and four square-root operations are required, which roughly scales as N^2 additions for large N .

It is interesting to compare these results with those for the Lanczos method where the highest and lowest eigenvalues are accurately determined, as outlined in Sect. 3. The computational bottleneck in this algorithm is the matrix–vector multiplication (which scales as N^2 multiplications) if the number of Krylov vectors is small compared to the size of the matrix. This results in a larger prefactor (as this method scales as N^2 multiplications as opposed to the N^2 additions for the method outlined in this paper) in scaling but yields exact eigenvalues as

opposed to bounds. It should be noted that the discussion here is for full matrices and that both methods display linear scaling for sparse matrices; the prefactor, however, remains the same as previously discussed.

5 Results

We now illustrate the results of Sect. 3 by first considering several particle-in-a-box-like systems, namely

1. An Eckart barrier in a one-dimensional box.
2. A Henon–Heiles well in a one-dimensional box.
3. A two-dimensional box with a two-dimensional Henon–Heiles well.

We next consider the well-studied problem of the ro-vibrational bound states of the H_3^+ molecular ion [32–36], and conclude this section with a study of a completely random, nonsymmetric matrix.

For the three particle-in-a-box-like systems, the KE part of the Hamiltonian was evaluated in the coordinate representation using the Hermite-distributed approximating functional (DAF) [37]. The (local) PE function was chosen to be positive semidefinite and it was added to the KE matrix to form the full (symmetric and positive definite) Hamiltonian matrix.

The eigenvalue bounds were calculated using Eqs. (24) and (25), and the results were compared with the exact eigenvalues obtained from direct diagonalization [38] of the Hamiltonian matrix. The eigenvalue bounds from Eqs. (24) and (25) were also compared (see Tables 1, 2) with

1. The bounds obtained from summing the separate maximum (or minimum) eigenvalues of the KE and PE matrices (the maximum and minimum eigenvalues of the KE matrix were obtained from direct diagonalization as seen in Tables 1 and 2 and the maximum and minimum eigenvalues of the PE were simply taken to be its maximum and minimum values, respectively, on the grid).
2. An estimate to the maximum (or minimum) eigenvalue of the KE (which was obtained using the solution to the particle-in-a-box problem) summed with the maximum (or minimum) PE on the grid.

In Tables 1 and 2, we also provide the maximum (minimum) PE on the grid, the maximum (minimum) element in the Hamiltonian matrix, and the Frobenius norm [18] along with a comparison of the upper and lower bound estimates obtained. The Frobenius norm and the maximum and minimum elements of the Hamiltonian are included simply because they have been used in the past to estimate spectral bounds. Clearly, they are not useful and are not recommended.

It is clear from Table 1 that the upper bound estimate from Eq. (25) is better than the estimated $\max(\text{KE}) + \max(\text{PE})$ for all the cases studied. The $\max(\text{KE}) + \max(\text{PE})$ (obtained using the actual maximum eigenvalue for the KE matrix from direct diagonalization), however, is better in the case of box 1, where the maximum value of the potential is much smaller than the

maximum KE (Table 1). In boxes 2 and 3, where the maximum values of the PE and KE are comparable (and the KE and PE commutator is larger than for box 1), $\max(\text{KE}) + \max(\text{PE})$ does not give as good an upper bound as Eq. (25) does. From Table 2, clearly, both estimated $\min(\text{KE}) + \min(\text{PE})$ and $\min(\text{KE}) + \min(\text{PE})$ provide better lower bounds than Eq. (24). The behavior of the upper and lower bounds as functions of c for the one-dimensional Henon–Heiles problem is shown in Fig. 1.

For the ro-vibrational bound states of the well-studied H_3^+ molecular ion [33–36], the KE part of the Hamiltonian was written in the Adiabatically Adjusting Principal Axis Hyperspherical (APH) [39] coordinate system to utilize the full symmetry of the potential, and was represented using symmetry-adapted DAFs (SADAFs) [40]. The PE part of the Hamiltonian was chosen

to be the Meyer, Botschwina and Burton potential [32]. Details regarding the SADAF representation and a discussion of the eigenvalues for H_3^+ obtained from this new approach, compared to previous work done on this benchmark system [33–36], can be found elsewhere [40]. Here we only consider the bounds on the eigenspectrum.

The SADAF representation of the APH KE operator is a nonsymmetric matrix [40]; however, the values of j_L and j_R in Eqs. (16)–(18) are the same for both $\|A\|_1$ and $\|A\|_\infty$, which forces α_1 to be equal to α_2 in this case. As a result, there are only two regions in this case (which is clear from Fig. 2) despite the Hamiltonian matrix being nonsymmetric. The behavior of the upper and lower bounds as a function of c is presented in Fig. 3. This behavior agrees with the analytical expressions in Eqs. (21)–(23). (The two seemingly flat regions in Fig. 3, namely, the upper bound for small c and the lower

Table 1. Upper bounds for the particle-in-a-box-like (self-adjoint) cases. The kinetic energy is represented by KE and the potential energy by PE

	Box 1 ^f	Box 2 ^g	Box 3 ^h
E_N^a	30.065462	111.390079	235.143910
$\text{Max}_j [H_{jj} + \sum_{i \neq j} H_{ij}]^b$	30.093964	117.899710	241.760585
Estimated $\text{Max}(\text{KE}) + \text{Max}(\text{PE})^c$	30.870730	130.933006	261.866012
$\text{Max}(\text{KE}) + \text{Max}(\text{PE})^d$	30.092883	129.382049	258.764098
$\text{Max}(\text{PE})$	0.028215	76.101868	152.203735
$\text{Max}_{i,j} H_{ij}$	10.512628	94.740825	189.481651
$\sqrt{\sum_{i=1}^m \sum_{j=1}^n H_{ij} ^2}^e$	548.100455	337.523545	5183.023934

^a Maximum eigenvalue as obtained from direct diagonalization of the discrete Hamiltonian matrix

^b Least upper bound from Eq. (25)

^c Estimated $\text{max}(\text{KE})$ obtained using the particle-in-a-box energy by setting the maximum quantum number as the number of grid points, i.e., estimated $\text{max}(\text{KE}) = \frac{\hbar^2 \pi^2}{2\mu \Delta x^2}$, for boxes 1 and 2 and estimated $\text{max}(\text{KE}) = \frac{\hbar^2 \pi^2}{2\mu \Delta x^2} + \frac{\hbar^2 \pi^2}{2\mu \Delta y^2}$ for box 3. $\text{Max}(\text{PE}) = V_{\text{max}}$, the maximum value of the potential on the grid. $\Delta x = 0.30$ a.u. for boxes 2 and 3, $\Delta y = \Delta x$ for box 3 and $\Delta x = 0.40$ a.u. for box 1. $\mu = 1$ a.u. for all cases

^d $\text{Max}(\text{KE})$ is obtained by actual diagonalization of the KE matrix. $\text{Max}(\text{PE}) = V_{\text{max}}$

^e Frobenius norm in Eq. (A10)

^f Eckart potential: $\frac{V_0}{\cosh^2(\frac{x-x_v}{a})}$ where $V_0 = 0.028215$ a.u., $x_v = 25.0$ a.u. and $a = 5$ a.u. Number of grid points = 1500. Grid range: -381 – 218.6 a.u.

^g One-dimensional Henon–Heiles potential: $\frac{1}{2}x^2 - \frac{\lambda}{3}x^3$, where $\lambda = \sqrt{0.0125}$. Number of grid points = 64

^h Two-dimensional Henon–Heiles potential: $\frac{1}{2}(x^2 + y^2) + \lambda(xy^2 - \frac{1}{3}x^3)$ where $\lambda = \sqrt{0.0125}$. Number of grid points = 64×64

Table 2. Lower bounds for the particle-in-a-box-like (self-adjoint) cases

	Box 1 ^c	Box 2 ^c	Box 3 ^c
E_1^a	0.0000296	0.498061	0.718253
$\text{Min}_j [H_{jj} - \sum_{i \neq j} H_{ij}]^b$	-9.096922	-16.161182	-32.322364
Estimated $\text{Min}(\text{KE}) + \text{Min}(\text{PE})^c$	0.0000137	0.024939	0.031043
$\text{Min}(\text{KE}) + \text{Min}(\text{PE})^d$	0.0000137	0.0242001	0.0484003
$\text{Min}(\text{PE})$	0	0.011124 ^f	0.022248 ^f
$\text{Min}_{i,j} H_{ij}$	-6.437512	-11.444467	-11.444467

^a Minimum eigenvalue as obtained from direct diagonalization of the discrete Hamiltonian matrix

^b Greatest lower bound from Eq. (24)

^c Estimated, per dimension, using estimated $\min(\text{KE}) = \frac{\hbar^2 \pi^2}{2\mu L^2}$, where L is the length of the box in the respective dimension. (Using particle-in-a-box energy with quantum number = 1.) $\text{Min}(\text{PE}) = V_{\text{min}}$, the minimum value of the potential on the grid

^d $\text{Min}(\text{KE})$ is obtained by actual diagonalization of the KE matrix. $\text{Min}(\text{PE}) = V_{\text{min}}$

^e Box parameters and forms of the potential as in Table 1

^f In boxes 2 and 3, there is no grid point at the potential minimum

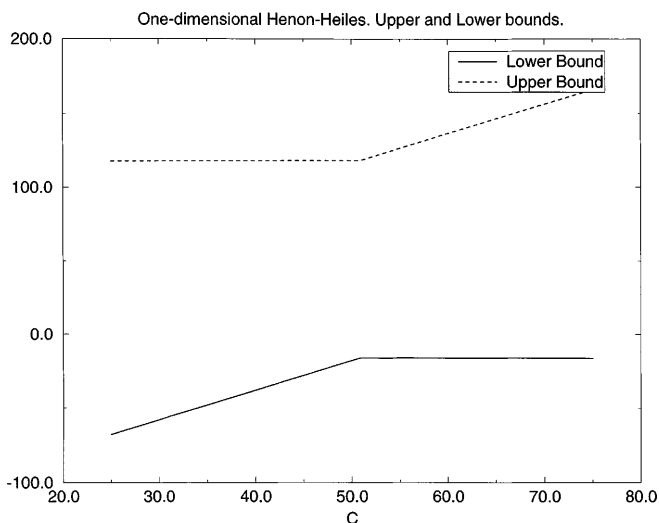


Fig. 1. A plot of $c + \sqrt{\|A\|_1 \|A\|_\infty}$ (dotted line) and $c - \sqrt{\|A\|_1 \|A\|_\infty}$ (solid line) as a function of c for the one-dimensional Henon–Heiles problem

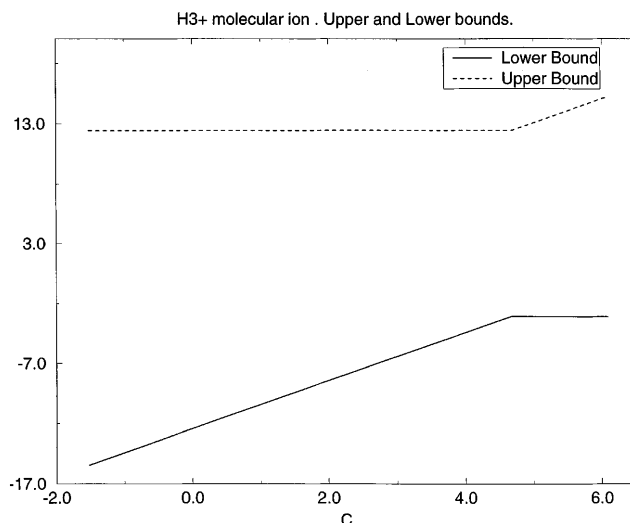


Fig. 3. A plot of $c + \sqrt{\|A\|_1 \|A\|_\infty}$ (dotted line) and $c - \sqrt{\|A\|_1 \|A\|_\infty}$ (solid line) as a function of c for the H_3^+ molecular ion with 900 grid points. The two seemingly flat regions in the asymptotic region of c , namely, the upper bound for small c and the lower bound for large c , are not really flat but have a small negative slope

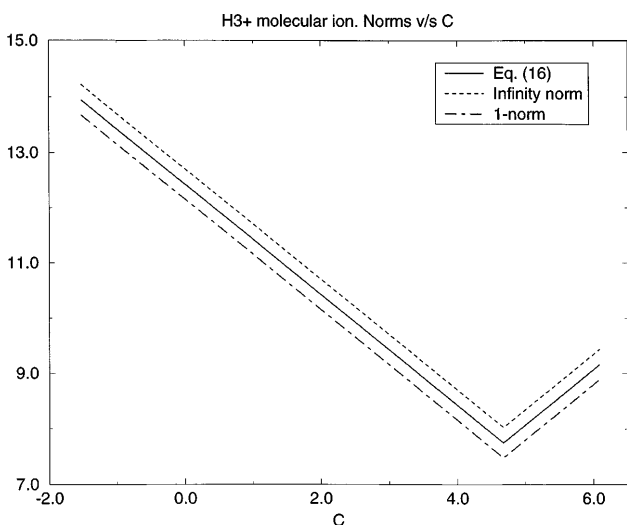


Fig. 2. A plot of the L^1 norm (dot-dash line), L^∞ norm (dotted line) and the geometric mean of the two as per Eq. (10) (solid line), for the matrix $A = H - cI$ as a function of c . This plot is for the H_3^+ molecular ion with 900 grid points

bound for large c , are actually not flat but have small negative slopes.) The upper and lower bounds were calculated at the point $c = \alpha_1 = \alpha_2$. In Table 3, we provide results for an A_1 irreducible representation Hamiltonian [40], and we compare these bounds with the maximum and minimum eigenvalues obtained from direct diagonalization, bounds obtained using Gerschgorin’s disk theorem, bounds obtained using the separate maximum and minimum eigenvalues of the KE and PE matrices, and the estimate obtained using the Frobenius norm. The results are shown for four different grid sizes. Clearly, $\min(\text{KE}) + \min(\text{PE})$ and $\max(\text{KE}) + \max(\text{PE})$ provide the best estimates, as $\max(\text{PE})$ is small compared to $\max(\text{KE})$ for all the cases studied and hence the KE and PE operator commutator tends to

be small. Calculation of $\min(\text{KE})$ and $\max(\text{KE})$, however, is nontrivial. Although in this study we employed the use of a direct diagonalization scheme to obtain these values, a Lanczos/Arnoldi-type [18, 29–37] method to obtain the outlying eigenvalues could be used here. In any case, the method shown in this paper provides a good upper bound at a very low computational cost, as seen in Sect. 4, and $\max(\text{KE}) + \max(\text{PE})$ is not guaranteed to give the best bound, as is seen in Table 1 for cases where the maximum value of the potential is comparable to the maximum KE, i.e., when the PE and KE commutator is not small). The next question one could raise is how does a “particle-in-a-box” estimate work for H_3^+ using the APH Hamiltonian? Unfortunately, in this case, it is not at all obvious how one constructs a model to estimate the maximum KE. In our opinion, this illustrates why our approach is attractive and useful. It is highly likely that different types of coordinates will be needed as one changes mass combinations and numbers of atoms in a system, and this would mean having to find a suitable model each time one considered a qualitatively different system. By contrast, the present approach provides excellent rigorous upper bounds and is trivially applied to any system, without any necessary modifications.

Still, we have found that the following model does provide an upper bound for the H_3^+ , APH Hamiltonian. For total angular momentum $J = 0$, the APH Hamiltonian may be written as

$$H = -\frac{\hbar^2}{2\mu} \frac{\partial^2}{\partial \rho^2} + \frac{15\hbar^2}{8\mu\rho^2} - \frac{\hbar^2}{2\mu\rho^2} \times \left[\frac{4}{\sin 2\theta} \frac{\partial}{\partial \theta} \sin 2\theta \frac{\partial}{\partial \theta} + \frac{1}{\sin^2 \theta} \frac{\partial^2}{\partial \chi^2} \right] + V. \quad (44)$$

One may obtain the upper bound to the eigenspectrum of this Hamiltonian as

Table 3. The H_3^+ molecular ion using the symmetry-adapted distributed approximating function representation

	1	2	3	4
N^a	900	1200	1600	2400
E_1^b	-0.165848	-0.165838	-0.165838	-0.165838
LUB at $c = \alpha_1 = \alpha_2^c$	-3.075203	-3.967688	-4.169539	-9.473521
$\text{Min}_j \left[H_{jj} - \sum_{i \neq j} H_{ij} \right]^d$	-3.353470	-4.356348	-4.578342	-10.548348
$\text{Min(KE)} + \text{Min(PE)}^e$	-0.184500	-0.184425	-0.184587	-0.184895
Min(PE)	-0.184959	-0.184889	-0.185056	-0.185364
$\text{Min}_{i,j} H_{ij}$	-3.352630	-4.304189	-4.527747	-10.175796
E_N^f	10.730040	13.787633	14.571956	32.555528
GLB at $c = \alpha_1 = \alpha_2^c$	12.418126	15.985873	16.941089	37.806993
$\text{Max}_j \left[H_{jj} + \sum_{i \neq j} H_{ij} \right]^d$	12.696394	16.374532	17.349892	38.881821
$\text{Max(KE)} + \text{Max(PE)}^e$	10.730067	13.787666	14.572019	32.555541
Max(PE)	0	0	0	0
$\sqrt{\sum_{i=1}^m \sum_{j=1}^n H_{ij} ^2}^g$	21.685648	30.142476	36.677676	80.722263
$\text{Max}_{i,j} H_{ij}$	4.671462	6.009092	6.385775	14.166736

^a Number of points on the three-dimensional hyperspherical grid

^b Lowest eigenvalue (a.u.) of the Hamiltonian matrix, obtained by direct diagonalization

^c Least upper bound (LUB) and greatest lower bound (GLB) estimates at $c = \alpha_1 = \alpha_2$, using the method described in Sect. 3

^d Bounds from Gerschgorin disk theorem [27, 28]. (Also see Sect. 3)

^e Max(KE) and min(KE) obtained from actual diagonalization of the KE matrix. Max(PE) and min(PE) are the maximum and minimum values of the potential on grid

^f Highest eigenvalue of the Hamiltonian matrix, obtained by direct diagonalization

^g Frobenius norm in Eq. (A10)

$$H_{\max} = V_{\max} + \frac{\pi^2 N_\rho^2}{2\mu(\rho_{\max} - \rho_{\min})^2} + \frac{\pi^2}{2\mu(\rho_{\min} \Delta\theta)^2} + \frac{\pi^2}{2\mu[\rho_{\min} \sin(\theta_{\min}) \Delta\chi]^2}, \quad (45)$$

where N_ρ is the number of grid points in ρ , chosen in the range $[\rho_{\min}, \rho_{\max}]$, $\Delta\theta$ and $\Delta\chi$ are the grid spacings along the θ and χ directions, θ_{\min} is the minimum value of θ on the grid and V_{\max} is the maximum value of the potential on the grid. The model clearly employs a ‘‘box length’’ equal to $[\rho_{\max} - \rho_{\min}]$ for the hyperradius, a box-length equal to $[\rho_{\min} \Delta\theta N_\theta]$ (where N_θ is the number of grid points in θ) for the motion along the θ variable, and a box length of $[\rho_{\min} \sin(\theta_{\min}) \Delta\chi N_\chi]$ for the motion along the χ variable, with N_χ being the number of grid points in χ . While it may be easy to justify the forms of the ρ KE, the θ and χ KEs are certainly ad hoc. Rather than use such an expression, it seems preferable to utilize a rigorous bound that also yields a better upper bound than the particle-in-a-box model. The model results are compared to our rigorous bounds in Table 4.

Non-Hermitian matrices arise in various problems in physical sciences, for example, the use of negative imaginary absorbing potentials in quantum scattering theory results in a non-Hermitian Hamiltonian matrix [41], the study of nonconservative systems often leads to a dynamical operator that is non-Hermitian, etc. Since the H_3^+ molecular ion problem, previously considered, is a ‘‘special’’ nonsymmetric matrix that exhibits only two regions, we tested the bounds for a nonsymmetric case whose elements were chosen randomly. The bounds for

Table 4. The H_3^+ molecular ion. Comparison of the LUB obtained at $c = \alpha_1 = \alpha_2$ with upper bounds from Eq. (45)

Box size	Max. eig.	LUB at $c = \alpha_1 = \alpha_2$	H_{\max} of Eq. (45)
900	10.73	12.418	14.251
1200	13.787	15.985	17.622
1600	14.571	16.941	17.826
2400	32.555	37.806	39.483

this matrix, as seen in Figs. 4 and 5, exhibit the expected three different regions; however, the upper and lower bounds calculated at α_1 and α_2 were not found to be as ‘‘tight’’ (see Table 5) for this random case as for the other cases studied. Unlike a quantum mechanical Hamiltonian matrix, a random matrix is not associated with a sum of KE and PE matrices, which have specific behavior dictated by physics. It is more difficult to estimate the bounds of a random matrix accurately than it is for the Hamiltonian matrix of a physical system. The method described in this paper has the virtue of yielding bounds for any matrix, random or not. Our experience is that the quality of the bounds is best when the matrix has a physical significance.

6 Conclusions

We have shown that the upper bound based on an estimate for the L^2 norm is computationally useful and yields better results, for situations where the PE may be comparable to the KE (i.e., when the respective

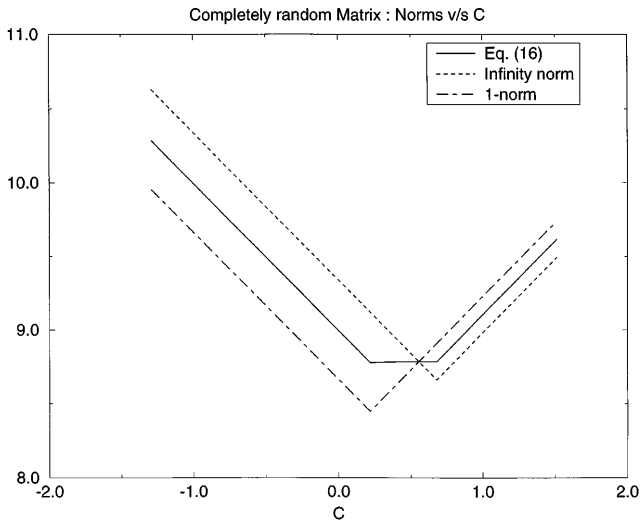


Fig. 4. A plot of the L^1 norm (dot-dash line), L^∞ norm (dotted line) and the geometric mean of the two as per Eq. (10) (solid line), for the matrix $\mathbf{A} = \mathbf{H} - c\mathbf{I}$ as a function of c . This plot is for the random non-self-adjoint matrix. The values for α_1 and α_2 were found to be 0.2187 and 0.6793, respectively. The graph clearly shows the existence of three regions: less than 0.2187, between 0.2187 and 0.6793, and greater than 0.6793

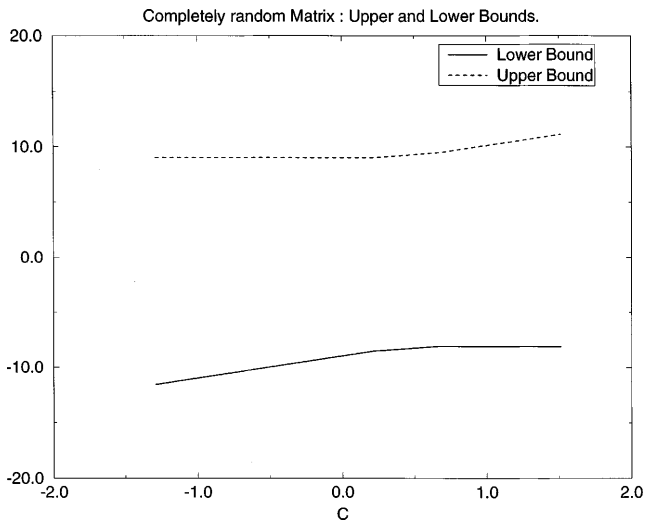


Fig. 5. A plot of $c + \sqrt{\|A\|_1 \|A\|_\infty}$ (dotted line) and $c - \sqrt{\|A\|_1 \|A\|_\infty}$ (solid line) as a function of c for the random non-self-adjoint matrix. The values for α_1 and α_2 were found to be 0.2187 and 0.6793, respectively

operators do not nearly commute), than that standardly obtained from summing the maximum exact KE and the maximum PE on the grid. When, however, the maximum PE is small compared to the maximum KE (i.e., when their commutator is likely to be small), the latter method yields better bounds. In the case of a realistic potential for the H_3^+ molecular ion the upper bound obtained is seen to be tight. The lower bound, on the other hand, obtained from summing the estimated minimum KE and the minimum value of the potential on the grid is found to be superior to that obtained using

Table 5. Random (non-self-adjoint) matrix

E_1^a	-1.258613 (real)
GLB of $c = \alpha_1$ or $c = \alpha_2^b$	-8.101976
$\text{Min}_j [H_{jj} - \sum_{i \neq j} H_{ij}]^c$	-7.97924
$\text{Min}_{i,j} H_{ij}$	-0.956900
E_N^d	2.052416
LUB of $c = \alpha_1$ or $c = \alpha_2^e$	8.994284
$\text{Max}_j [H_{jj} + \sum_{i \neq j} H_{ij}]^c$	9.337762
$\text{Max}_{i,j} H_{ij}$	0.990727
$\sqrt{\sum_{i=1}^m \sum_{j=1}^n H_{ij} ^2}$	8.455413

^a Minimum eigenvalue

^b The greater of the two bound values calculated at α_1 and α_2

^c Bounds from Gerschgorin disk theorem [27, 28]

^d Maximum eigenvalue

^e The lesser of the two bound values calculated at α_1 and α_2

the estimate based on the L^2 norm. Since one is free to use the least upper bound and the greatest the lower bound, one can simply normalize the spectrum of the matrix using the best of each bounds, regardless of whether they were obtained by the same technique. The comparisons with the eigenvalues of the KE and potential matrices, of course, apply only to the specific case of Hamiltonian matrices. However, the estimate of bounds using the L^2 norm is applicable to any matrix. The H_3^+ case shows clearly that the present method is preferable to the use of ad hoc models such as the particle-in-a-box method, which really is useful only in the case of Cartesian-like variables. When the coordinate transformation complicates the KE, it seems much better to use an approach which not only yields a rigorous upper bound, and which is always applied in the same manner no matter what sort of coordinates are employed, but which also requires very little computational effort.

We believe this method will be useful in normalizing the Hamiltonian matrix, as is required for use in various Cheychev propagations and filter diagonalizations.

Acknowledgements. S.S.I. would like to thank Stephen Gray at the Argonne National Laboratories for helpful comments and for directing our attention to Gerschgorin's theorem. He also acknowledges Stuart Althorpe and Guowei Wei for their helpful comments. S.S.I. is supported in part under R. A. Welch Foundation grant E-0608. Acknowledgment is made to the donors of the Petroleum Research Foundation by the American Chemical Society, for partial support of this research. D.J.K. is supported, in part, under National Science Foundation grant CHE-9700297. The Ames Laboratory is operated for the Department of Energy by Iowa State University under contract no. 2-7405-ENG82.

Appendix 1. The L^1 and L^∞ norms

Consider the L^∞ norm of the $m \times n$ rectangular matrix, \mathbf{A} . According to Eq. (4), the set of all vectors satisfying the normalization condition $\|x\|_\infty = 1$ is determined by $0 \leq |x_k| \leq 1$ for $k = 1$ to n . From this it follows that

$$(Ax)_i = \sum_{j=1}^n A_{ij}x_j \leq \sum_{j=1}^n |A_{ij}| \quad (\text{A1})$$

for any vector \mathbf{x} normalized according to Eq. (4). Since the components of the vector \mathbf{x} for each value of i can be chosen arbitrarily close to $\frac{A_{ij}^*}{|A_{ij}|}$, in which case the last relation of Eq. (A1) becomes an equality, it follows that

$$\|A\|_\infty = \max_{1 \leq i \leq m} \sum_{j=1}^n |A_{ij}|, \quad (\text{A2})$$

Similarly, from Eq. (2) the L^1 norm of \mathbf{A} can be obtained from the series of relationships

$$\begin{aligned} \|A\|_1 &= \max_{\|\mathbf{x}\|_1=1} \|Ax\|_1 = \max_{\|\mathbf{x}\|_1=1} \sum_{i=1}^m \left| \sum_{j=1}^n A_{ij}x_j \right| \\ &\leq \max_{\|\mathbf{x}\|_1=1} \sum_{i=1}^m \sum_{j=1}^n |A_{ij}| |x_j| = \max_{\|\mathbf{x}\|_1=1} \sum_{j=1}^n \sum_{i=1}^m |A_{ij}| |x_j|. \end{aligned} \quad (\text{A3})$$

However,

$$\begin{aligned} &\max_{\|\mathbf{x}\|_1=1} \sum_{j=1}^n \left[\sum_{i=1}^m |A_{ij}| \right] |x_j| \\ &\leq \max_{\|\mathbf{x}\|_1=1} \sum_{j=1}^n \left[\sum_{i=1}^m |A_{ij^*}| \right] |x_j| = \sum_{i=1}^m |A_{ij^*}|, \end{aligned} \quad (\text{A4})$$

where j^* is the value of j that maximizes $\sum_{i=1}^m |A_{ij^*}|$, and we have made use of the fact that $\|\mathbf{x}\|_1 = 1$. Since

$$\|A\|_1 = \sum_{i=1}^m |A_{ij^*}|$$

for $x_j = \delta_{jj^*}$, it follows that

$$\|A\|_1 = \sum_{i=1}^m |A_{ij^*}| = \max_{1 \leq j \leq n} \sum_{i=1}^m |A_{ij}|. \quad (\text{A5})$$

Appendix 2: Relations between the L^1 , L^∞ and L^2 norms

Consider the L^1 norm of Eq. (9) to obtain

$$|\mu|^2 \|z\|_1 = \|A^\dagger Az\|_1 \leq \|A^\dagger\|_1 \|A\|_1 \|z\|_1, \quad (\text{A6})$$

where we have used the Schwartz inequality [42]. From Eqs. (6) and (7), it is clear that

$$\|A^\dagger\|_1 = \max_{1 \leq j \leq m} \sum_{i=1}^n |A_{ij}^\dagger| = \max_{1 \leq j \leq m} \sum_{i=1}^n |A_{ji}| = \|A\|_\infty. \quad (\text{A7})$$

Using this result in Eq. (A6) we obtain

$$|\mu|^2 \|z\|_1 \leq \|A\|_\infty \|A\|_1 \|z\|_1, \quad (\text{A8})$$

which proves the inequality

$$\|A\|_2 \leq \sqrt{\|A\|_1 \|A\|_\infty}. \quad (\text{A9})$$

There exists a variety of other ways to estimate an upper bound for the L^2 norm of a matrix [18]. Although we study only the expression provided in Eq. (A9), for the sake of completeness, we also give a few of the other expressions found in the literature.

$$\|A\|_2 \leq \|A\|_F \leq \sqrt{n} \|A\|_2 \quad (\text{A10})$$

where, $\|A\|_F$ is the Frobenius norm given by

$$\begin{aligned} \|A\|_F &= \sqrt{\sum_{i=1}^m \sum_{j=1}^n |a_{ij}|^2}, \\ \max_{i,j} |a_{ij}| &\leq \|A\|_2 \leq \sqrt{mn} \max_{i,j} |a_{ij}| \end{aligned} \quad (\text{A11})$$

$$\frac{1}{\sqrt{n}} \|A\|_\infty \leq \|A\|_2 \leq \sqrt{m} \|A\|_\infty \quad (\text{A12})$$

$$\frac{1}{\sqrt{m}} \|A\|_1 \leq \|A\|_2 \leq \sqrt{n} \|A\|_1. \quad (\text{A13})$$

Appendix 3: Greatest lower bound and least upper bound for the spectrum of \mathbf{H} in the three regions of c

We consider the slopes of the upper and lower bounds in the three regions described by Eqs. (21)–(23). If we

define $x = \sqrt{\frac{|c - \alpha_2| + \beta_2}{|c - \alpha_1| + \beta_1}}$, then for $c \leq \alpha_1$, Eq. (21)

yields

$$\frac{d}{dc} \left[c \pm \sqrt{\|A\|_1 \|A\|_\infty} \right] = 1 \mp \frac{1}{2} \left[x + \frac{1}{x} \right] \quad (\text{A14})$$

Since the quantity $\frac{1}{2} \left[x + \frac{1}{x} \right] \geq 1$ for all positive values of x , the slope of the upper bound is either zero or negative, and that of the lower bound is always positive in this region. Therefore, the greatest lower bound and the least upper bound in the region $c \leq \alpha_1$ are at $c = \alpha_1$. For the special case of a self-adjoint matrix, $\alpha_1 = \alpha_2$ and hence $x = 1$. Therefore, the slope of the upper bound, in this case, is zero for all $c \leq \alpha_1$, and the least upper bound is constant in this region.

For $c \geq \alpha_2$, differentiating Eq. (23), we obtain

$$\frac{d}{dc} \left[c \pm \sqrt{\|A\|_1 \|A\|_\infty} \right] = 1 \pm \frac{1}{2} \left[x + \frac{1}{x} \right]. \quad (\text{A15})$$

Following the same argument as before, we find that the slope of the upper bound is always positive, and the slope of the lower bound is negative or zero, in this region. Hence, the greatest lower bound and the least upper bound here are at $c = \alpha_2$. For the self-adjoint case, the slope of the lower bound is zero and hence the lower bound is constant in this region.

For $\alpha_1 < c < \alpha_2$

$$\begin{aligned} c \pm \sqrt{(c - \alpha_1 + \beta_1)(\alpha_2 - c + \beta_2)} &= c \pm \sqrt{(c - c_1)(c_u - c)} \\ &= c - y(c - c_1), \end{aligned} \quad (\text{A16})$$

where $c_u = \alpha_2 + \beta_2$, $c_l = \alpha_1 - \beta_1$, $y = \mp x$ and x has the same definition as before. Clearly, the quantity y is positive for the lower bound and negative for the upper bound. Furthermore, the bound values are real when c lies in $[c_l, c_u]$, which, by definition, extends outside the region $[\alpha_1, \alpha_2]$. Differentiating the above expression, we find

$$\frac{d}{dc} \left[c \pm \sqrt{\|A\|_1 \|A\|_\infty} \right] = 1 - \frac{1}{2} \left[y - \frac{1}{y} \right], \quad (\text{A17})$$

which has roots at $y = 1 + \sqrt{2}$ and $y = 1 - \sqrt{2}$. The first root is positive and hence determines the extremum for the lower bound, while the second root, being negative, determines the extremum for the upper bound; however, the root at $y = 1 + \sqrt{2}$ corresponds to a minimum, and the root at $y = 1 - \sqrt{2}$ corresponds to a maximum, and hence, the behavior for the upper bound is convex upwards and the behavior for the lower bound is convex downwards in the region $c_l < c < c_u$. Consequently the bound estimates in this region are never better than those at the edges, i.e., at the points $c = \alpha_1$ and $c = \alpha_2$.

References

- Nauts A, Wyatt RE (1983) Phys Rev Lett 51: 2238
- Tal-Ezer H, Kosloff R (1984) J Chem Phys 81: 3967
- Mowrey RC, Kouri DJ (1986) J Chem Phys 84: 6466
- Zhu W, Huang Y, Kouri DJ, Chandler C, Hoffman DK (1994) Chem Phys Lett 217: 73
- Parker GA, Zhu W, Huang Y, Hoffman DK, Kouri DJ (1996) Comput Phys Commun 96: 27
- Huang Y, Kouri DJ, Hoffman DK (1999) J Chem Phys 110: 8303
- Neuhauser D (1994) J Chem Phys 100: 5076
- Chen R, Guo H (1997) Chem Phys Lett 277: 191
- Mandelshtam VA, Taylor HS, Miller WH (1996) J Chem Phys 105: 496
- Kouri DJ, Arnold M, Hoffman DK (1993) Chem Phys Lett 203: 166
- (a) Huang Y, Zhu W, Kouri DJ, Hoffman DK (1993) Chem Phys Lett 206: 96; (b) Huang Y, Zhu W, Kouri DJ, Hoffman DK (1993) Chem Phys Lett 213: 209
- Hoffman DK, Huang Y, Zhu W, Kouri DJ (1994) J Chem Phys 101: 1242
- Kouri DJ, Huang Y, Zhu W, Hoffman DK (1994) J Chem Phys 100: 3662
- Zhu W, Huang Y, Kouri DJ, Arnold M, Hoffman DK (1994) Phys Rev Lett 72: 1310
- Jang HW, Light JC (1995) J Chem Phys 102: 3262
- Huang Y, Iyengar SS, Kouri DJ, Hoffman DK (1996) J Chem Phys 105: 927
- (a) Hartke B, Kosloff R, Ruhman S (1986) Chem Phys Lett 158: 223; (b) Baer R, Kosloff R (1992) Chem Phys Lett 200: 183
- Golub GH, van Loan CF (1996) Matrix computations. The Johns Hopkins University Press, Baltimore
- Temple G (1928) Proc R Soc Lond Ser A 119: 276
- Bazley NW (1960) Phys Rev 120: 144
- Gay JG (1964) Phys Rev 135: A1220
- (a) Löwdin P-O (1965) Phys Rev 139: A357; (b) Löwdin P-O (1965) J Chem Phys 43: S175
- Eckart C (1930) Phys Rev 36: 878
- (a) Miller WH (1965) J Chem Phys 42: 4305; (b) Wilson EB Jr (1965) J Chem Phys 42: S172
- Miller WH (1968) J Chem Phys 48: 530
- Gordon RG (1968) J Chem Phys 48: 4984
- Varga RS (1963) Matrix iterative analysis. Prentice Hall, Englewood Cliffs
- Gradshteyn IS, Ryzhik IM (1980) Table of integrals, series, and products. Academic, New York
- Lanczos C (1950) J Res Natl Bur Stand 45: 255
- Sorensen DC (1992) SIAM J Matr Anal Apps 13: 357
- Parlett BN, Saad Y (1987) Linear Algebra Applications vol 88/89, pp 575–595
- Meyer W, Botschwina P, Burton PG (1986) J Chem Phys 84: 891
- Tennyson J, Henderson JR (1989) J Chem Phys 91: 3815
- Brass O, Tennyson J, Pollak E (1990) J Chem Phys 92: 3377
- Tennyson J, Brass O, Pollak E (1990) J Chem Phys 92: 3005
- Bacic Z, Zhang JZH (1991) Chem Phys Lett 184: 513
- Hoffman DK, Nayar N, Sharafeddin OA, Kouri DJ, J Phys Chem 95: 8299
- Anderson E, Bai Z, Bischof CH, Demmel J, Dongarra JJ, Du Croz J, Greenbaum A, Hammarling S, Mckenney A, Ostrouchov S, Sorensen DC (1992) LAPACK users guide, SIAM, Philadelphia
- Pack RT, Parker GA (1987) J Chem Phys 87: 3888
- Iyengar SS, Parker GA, Kouri DJ, Hoffman DK (1999) J Chem Phys 110: 10283
- Neuhauser D, Judson RS, Baer M, Kouri DJ (1994) in: Bowman JM (ed) Advances in molecular vibrations and collision dynamics, vol 2B. Jai Press, Greenwich, Conn., pp 27–44
- Riesz F, Sz-Nagy B (1990) Functional analysis. Dover New York